Polarimetric Interferometry

Martin Hellmann[1], Shane R. Cloude[2]

[1]German Aerospace Center (DLR), VO-ST, Linder Höhe, D-51140 Köln, Germany,
e-mail: martin.hellmann@dlr.de
[2]Shane R Cloude, e-mail: scloude@ieee.org

Abstract

This lecture presents the role of Polarimetry in SAR Interferometry. A general formulation for vector wave interferometry is presented that includes conventional scalar interferometry presented in the respective former lecture as a special case. Based on this formulation, the coherence optimization problem can be solved to obtain the optimum scattering mechanisms that lead to the best phase estimates. Comparison with conventional single-polarization estimates illustrates the significant processing gains that are possible if there is access to full polarimetric interferometric data. A comparison with conventional single-polarization presented in former lectures illustrates the significant processing gains that are possible if access to full polarimetric interferometric data is possible. The strong polarization dependence of the coherence will be addressed and the analytical solution for optimum polarization states that maximize the interferometric coherence will be derived and applied to experimental data. These improved interferogrammes allow an improvement of the accuracy of derived DEM products.

The introduction of a new coherent decomposition theorem for interferometric applications based on the Singular value spectrum of a 3 x 3 complex matrix allows the decomposition of polarimetric interferometric problems into a set of coherent scattering mechanisms. As a consequence, it is possible to generate interferograms related to certain independent scattering mechanisms and extract the height differences between them. The limitation of this technique is the existence of independent scattering mechanisms located at different height positions.

To explain the physical origin of these mechanisms, a coherent electromagnetic scattering model will be established which, additionally, can be used to establish the suitability of the decomposition algorithm for solving the problem of estimating the location of the effective scattering center, which is a critical point in the physical interpretation of interferograms. However, these introduction of Polarimetry in interferometric processing requires that fully coherent polarimetric data must be collected in order to separate the scattering mechanisms.. In this connection polarimetric Differential Interferometry will be considered also.

The phase difference between the optimum interferograms obtained by the application of the algorithm on the SIR-C data turned out to be strongly correlated with the actual forest height. This was a major result indicating the potential of the coherent combination of polarimetry and interferometry.

Introduction

Polarimetric SAR Interferometry was a first step in the abatement of the scattering ambiguity problem in the height direction. By combining interferometric and polarimetric techniques, it enables the separation of different scattering mechanisms within a resolution cell and at the same time, the estimation of the associated heights. Both, radar polarimetry and radar interferometry are phase sensitive techniques. The use of polarimetric SAR data has been widely addressed in the last decade. The tight relation between natural media physical properties and their polarimetric features leads to highly descriptive results that can be interpreted by analyzing underlying scattering mechanisms. Interferometric data on the other hand provide information concerning the coherence of the scattering mechanisms and can be used to retrieve observed media structures and complexity. The complementary aspect of polarimetric

Hellmann, M.; Cloude, S.R. (2007) Polarimetric Interferometry. In *Radar Polarimetry and Interferometry* (pp. 8-1 – 8-14). Educational Notes RTO-EN-SET-081bis, Paper 8. Neuilly-sur-Seine, France: RTO. Available from: http://www.rto.nato.int/abstracts.asp.

Report Documentation Page

Form Approved
OMB No. 0704-0188

1. REPORT DATE	2. REPORT TYPE	3. DATES COVERED
01 FEB 2007	**N/A**	**-**

4. TITLE AND SUBTITLE	5a. CONTRACT NUMBER
Polarimetric Interferometry	5b. GRANT NUMBER
	5c. PROGRAM ELEMENT NUMBER
6. AUTHOR(S)	5d. PROJECT NUMBER
	5e. TASK NUMBER
	5f. WORK UNIT NUMBER
7. PERFORMING ORGANIZATION NAME(S) AND ADDRESS(ES) **German Aerospace Center (DLR), VO-ST, Linder Höhe, D-51140 Köln, Germany**	8. PERFORMING ORGANIZATION REPORT NUMBER
9. SPONSORING/MONITORING AGENCY NAME(S) AND ADDRESS(ES)	10. SPONSOR/MONITOR'S ACRONYM(S)
	11. SPONSOR/MONITOR'S REPORT NUMBER(S)

12. DISTRIBUTION/AVAILABILITY STATEMENT
Approved for public release, distribution unlimited

13. SUPPLEMENTARY NOTES
See also ADM001954., The original document contains color images.

14. ABSTRACT

15. SUBJECT TERMS

16. SECURITY CLASSIFICATION OF:			17. LIMITATION OF ABSTRACT	18. NUMBER OF PAGES	19a. NAME OF RESPONSIBLE PERSON
a. REPORT	b. ABSTRACT	c. THIS PAGE			
unclassified	**unclassified**	**unclassified**	**UU**	**14**	

and interferometric information leads to a combination of both approaches. In 'Polarimetric-Interferometric Synthetic Aperture Radar (POL-INSAR) Imaging' it is possible to recover textural and spatial properties simultaneously. This includes the extraction of 'Digital Elevation Maps (DEM)' from either 'fully Polarimetric (scattering matrix) or interferometric SAR image data takes' with the additional benefit of obtaining co-registered three-dimensional 'POL-IN-DEM' information.

Over the next few years several free-flying remote sensing satellites will be deployed in orbit, providing the international scientific, commercial and military communities with a wealth of new data. Many of these will carry advanced multi-channel imaging radars designed to combine various levels of polarisation diversity with radar interferometry.

Polarimetric interferometry has proved to be a valuable tool for many applications. One is remote sensing where it has been shown in several recent publications that by using interferograms in multiple polarisation channels, estimation of vegetation height, underlying ground topography and mean extinction is possible [11,14,23].

Polarimetric Synthetic Aperture Radar interferometry (POLInSAR) can also be used to enhance the detection of military targets hidden beneath foliage. The key idea is to note that for random volume scattering the interferometric coherence is invariant to changes in wave polarisation. On the other hand, in the presence of a target the coherence changes with polarisation. It can be shown that under general symmetry constraints this change is linear in the complex coherence plane. These observations can be used to devise a filter to suppress the returns from foliage clutter while maintaining the signal from hidden targets.

Radar Polarimetry

As shown in a previous lecture, an important extension to single-channel SAR remote sensing is the utilisation of polarised waves. A polarimetric SAR system measures the electric field, backscattered by the scene, including its polarisation state. The interaction of the transmitted wave with a scattering object transforms its polarisation.

One special characteristic of SAR polarimetry is that it allows a discrimination of different types of scattering mechanisms. This becomes possible because the observed polarimetric signatures depend strongly on the actual scattering process. In comparison to conventional single-channel SAR, the inclusion of SAR polarimetry consequently can lead to a significant improvement in the quality of data analysis. Certain polarimetric scattering models even provide a direct physical interpretation of the scattering process, allowing an estimation of physical ground parameters like soil moisture and surface roughness [11], as well as unsupervised classification methods with automatic identification of different scatterer characteristics and target types [4,5].

SAR polarimetry additionally offers some limited capability for separating multiple scattering mechanisms occurring inside the same resolution cell and can be deemed as a first step in resolving the ambiguous scattering problem in SAR, as mentioned above. With polarimetric decomposition techniques a received signal can be split into a sum of three scattering contributions with orthogonal polarimetric signatures. This can be used for extracting the corresponding target types in the image, even in the case that they are occurring superimposed. Also, if a signal is disturbed by undesired orthogonal contributions, in this way the relevant components can be extracted.

The Phase

In radar polarimetry [1] we analyze the shape of the transmit (and receive) polarisation ellipse, as shown schematically in Figure 1a, for the purposes of improved information extraction. Figure 1a shows the spatial helix resulting from a combination of horizontal (H, in green) and vertical (V, in blue) transmitted components.

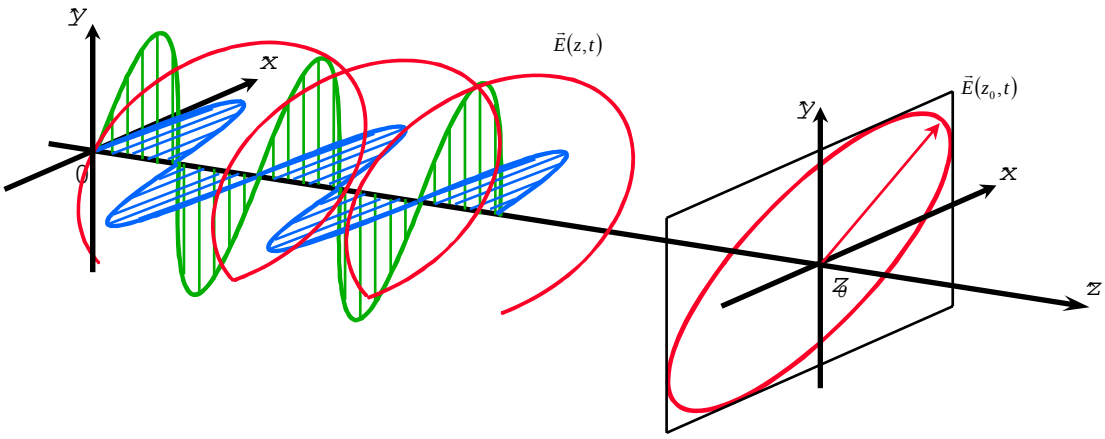

Figure 1a : The Polarisation Ellipse and Spatial helix decomposed into orthogonal components x (horizontal H) and y (vertical V) [Pottier, lectures on polarimetry]

By controlling the relative amplitudes we can rotate the polarisation from H through 45 degrees to V. However, by adjusting the relative timing (phase) of the blue and green components we can also adjust the shape of the ellipse as shown in Figure 1b. It is this combined amplitude and phase dimension that leads to increased information content in remote sensing applications, since the level of scattering we observe from natural terrain depends on the shape of this ellipse. [1,2,3,4,5]

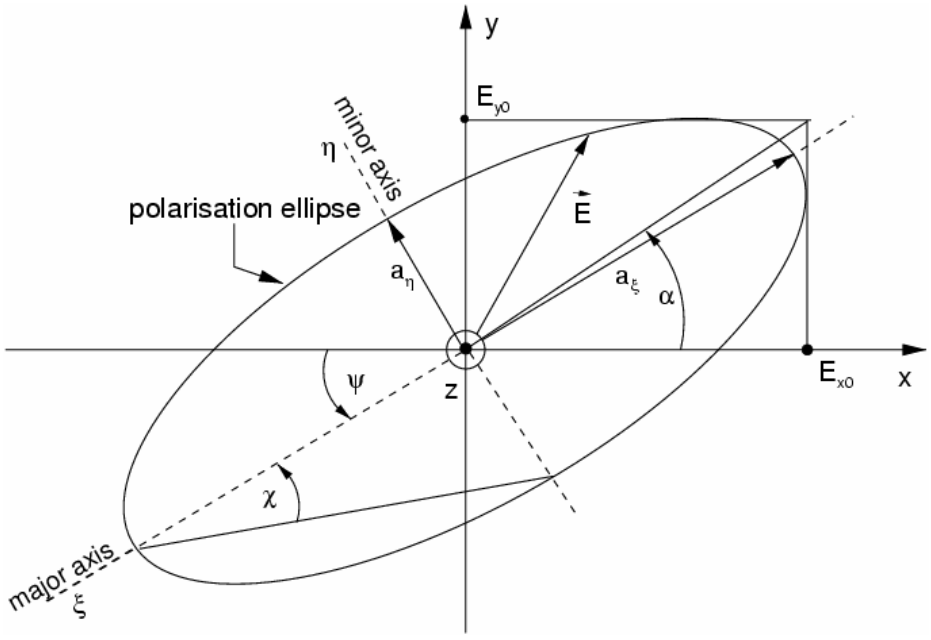

Figure 1b : The Polarisation Ellipse

To represent this combined amplitude and phase control mathematically, we describe the wave using a pair of complex numbers, e_x and e_y as shown in equation 1. The phase difference i.e. $\varphi = \arg(e_x e_y^*)$ then controls the shape of the ellipse, with linear polarisations defined by $\varphi = 0$. Note that the ellipse is actually a dynamic quantity, being the time locus of the helix in a fixed spatial plane. Consequently the locus can move clockwise or counter-clockwise (when viewed in the –z direction), corresponding to what are termed left and right-handed polarisations respectively. The set of all possible left and right handed ellipses can then be conveniently mapped onto the northern and southern hemispheres of the Poincaré sphere. Figure 1c [1,6]

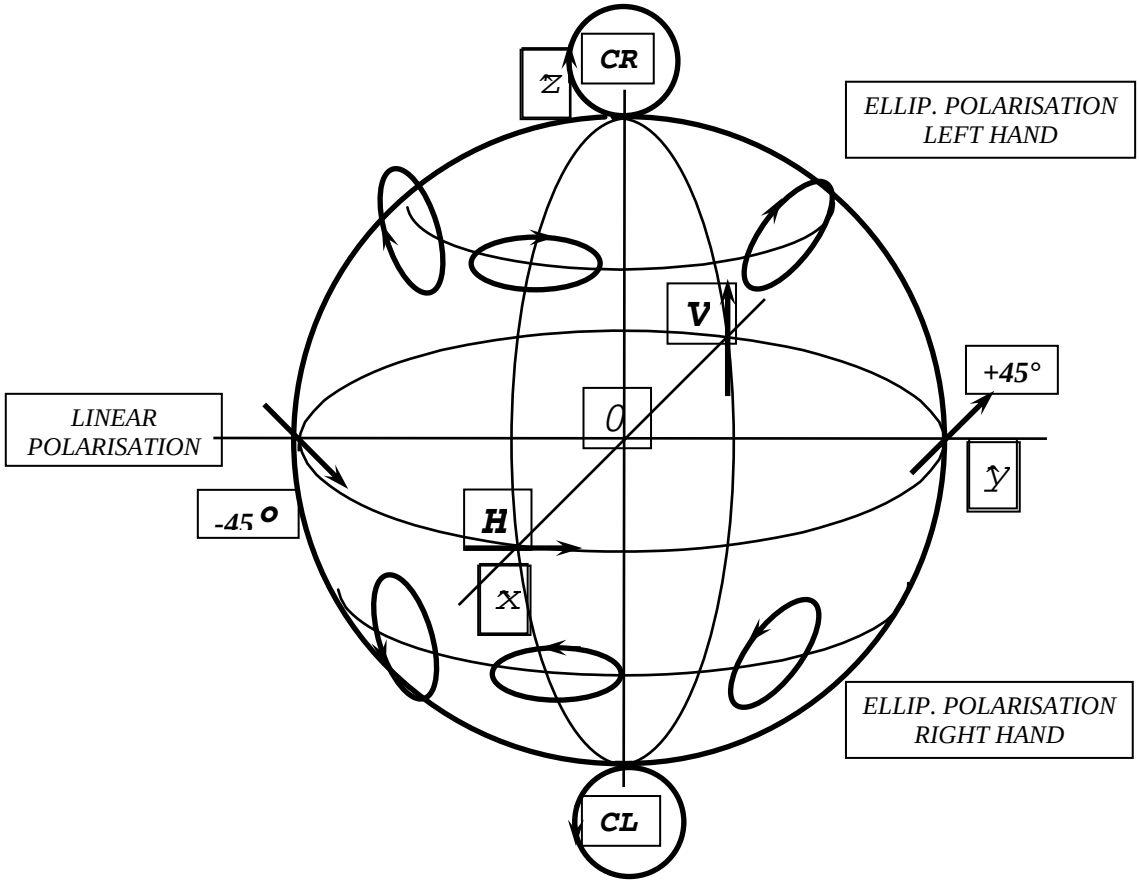

Figure 1c : The Poincaré sphere

Furthermore, our ability to extract quantitative information rests on the stability of this phase or the robustness of the spatial helix to small time and spatial shifts. A generic way to define the stability of this helix is to use the wave coherency matrix [J], taken at a point in space with position vector r. and formed as an average of all possible complex products between e_x and e_y as shown in equation 1, [6]

$$e_x\hat{x} + e_y\hat{y} \Rightarrow \underline{E} = \begin{bmatrix} e_x \\ e_y \end{bmatrix} \Rightarrow [J] = \left\langle \underline{E}.\underline{E}^{*T} \right\rangle = \begin{bmatrix} \left\langle e_x(\underline{r})e_x^*(\underline{r}) \right\rangle & \left\langle e_x(\underline{r})e_y^*(\underline{r}) \right\rangle \\ \left\langle e_y(\underline{r})e_x^*(\underline{r}) \right\rangle & \left\langle e_y(\underline{r})e_y^*(\underline{r}) \right\rangle \end{bmatrix} \quad (1)$$

As its name suggests, this matrix allows us to calculate not only the wave intensity (from the diagonal components) but also the coherence, which is a measure of the phase stability of the wave, as defined in equation 2 [7].

$$\tilde{\gamma}_{xy} = \frac{\left\langle e_x(\underline{r}) e_y^*(\underline{r}) \right\rangle}{\sqrt{\left\langle e_x(\underline{r}) e_x^*(\underline{r}) \right\rangle . \left\langle e_y(\underline{r}) e_y^*(\underline{r}) \right\rangle}}, 0 \le \left|\tilde{\gamma}_{xy}\right| \le 1 \tag{2}$$

A key benefit of employing ratios such as equation 2 is that absolute amplitude terms cancel, so removing some of the structural dependence in scattering from random media. It is this observation that shifts interest in polarimetry towards the study of ratios as potentially more robust indicators of physical structure (see examples in table I).

In active microwave sensing we assume $\left|\tilde{\gamma}_{xy}\right| = 1$ for the transmitted wave and hence the transmitted spatial helix is very stable. However, when the wave is scattered or reflected from natural media, its phase and amplitude will in general be modified (as shown schematically in Figure 2a). This process again must be described by a set of complex numbers, this time by a set of four, being the elements of the coherent scattering matrix [S] defined as shown in equation 3. This matrix characterises all possible phase and amplitude changes due to copolar (diagonal elements) and cross-polar (off diagonal) scattering. In practice, for the common case of backscatter, the reciprocity theorem for electromagnetic waves reduces this set to three complex numbers, as the cross-polarisation terms are equal $S_{HV} = S_{VH}$. Note that while this is widely true, there are a few special but important cases where it breaks down, as for example in low frequency radio wave propagation through the ionosphere, where the earths magnetic field lines break this reciprocity symmetry and as a result the cross polarisation terms are no longer equal. This observation can be used to calibrate the effects of Faraday rotation due to trans-ionospheric propagation, an important issue for the deployment of low frequency space-borne radars [8].

$$\underline{E}_s = \frac{e^{ikr}}{r}[S]\underline{E} \Rightarrow [S] = \begin{bmatrix} S_{HH} & S_{HV} \\ S_{VH} & S_{VV} \end{bmatrix} \xrightarrow[S_{HV}=S_{VH}]{reciprocity} \underline{k} = \begin{bmatrix} S_{HH} \\ \sqrt{2}S_{HV} \\ S_{VV} \end{bmatrix} \Rightarrow [C] = \left\langle \underline{k}.\underline{k}^{*T} \right\rangle \tag{3}$$

One key idea in polarimetry is that if we know all four of these [S] matrix elements then we can calculate the phase stability of the scattered signal for arbitrary incident ellipse, using a 3 x3 covariance matrix [C] as shown in equation 3. In this way we don't have to actually change the shape of the transmit ellipse (which would call for control of the antenna and microwave electronics) but can simulate the same effect off-line in the processing stages. For this reason there has been a lot of interest in the development of microwave switching systems that are capable of measuring all four elements of [S] (the simplest is to switch each transmit pulse between X and Y orthogonal polarisations with simultaneous reception of the X and Y components). Note that one important step is to calibrate system distortion effects due to crosstalk (which causes problems with estimation of the off-diagonal elements of [S]) and channel imbalance due to phase and amplitude distortions of the radar system itself. The development of robust calibration procedures has been a key enabling step in the quantitative exploitation of this technology [9]. Such systems are called 'quadpol' as they measure 4 complex numbers for each pixel in the image and allow the user to explore the whole Poincaré sphere. There are currently several mature airborne quadpol radar sensors with such a capability, but significantly there will soon be a new generation of free-flying satellite radars operating in this mode. The European Terrasar-X/L, Japanese ALOS-PALSAR and Canadian Radarsat-2 are important examples. The main question then becomes, how can we find the best polarisation combination to derive information

products exploiting the scattering of waves from surfaces and vegetation? To answer this we must look more carefully at equation 2 and the whole issue of coherence.

Coherence and Entropy

To calculate polarimetric coherence, we first choose a pair of polarisations x and y, then measure the (complex) components of the signal in these two channels and estimate the coherence by averaging. However, even for a fixed wave, the coherence obtained with this method will depend on the choice of our reference pair x and y (e.g. choosing x=y will give a coherence of 1, while less obvious but more important is the idea that for every wave we can choose an orthogonal pair x and y so that the coherence is zero). This goes against the idea that the spatial helix is somehow independent of the co-ordinates we use to represent it, and that consequently we should be able to describe its stability in co-ordinate invariant terms. One way to do this is to describe the helix stability using a generalised coherence or entropy (another popular way is to use the degree of polarisation [6]). The wave entropy is formally defined from the ratio of eigenvalues of [J] (see equation 4) and has a value of 0 when the helix is perfectly stable and 1 when it becomes noise like [2,4,6].

$$0 \le H_w = -\sum_{i=1}^{2} p_i \log_2 p_i \le 1, \quad p_i = \frac{\lambda_i([J])}{\sum \lambda} \tag{4}$$

By extension, we can also describe the loss of helix stability after scattering by the entropy of the 3 x3 covariance matrix [C] in equation 3, as defined in equation 5 [2,4]

$$0 \le H_s = -\sum_{i=1}^{3} p_i \log_3 p_i \le 1, \quad p_i = \frac{\lambda_i([C])}{\sum \lambda} \tag{5}$$

It is important to realize that this scattering entropy is characteristic of the scattering medium itself. For example, for low frequency volume scattering from a cloud of ellipsoidal particles of dielectric constant ε_r and axial ratio m, the normalized eigenvalues of [C] can be evaluated explicitly as shown in equation 6 [2,4,16,17]

$$m = \begin{cases} >1 \ \text{prolate particles} \\ 1 \ \text{spherical particles} \\ <1 \ \text{oblate particles} \end{cases} \Rightarrow R = \frac{m\varepsilon_r + 2}{m + \varepsilon_r + 1} \Rightarrow \begin{cases} \lambda_1 = 2R^2 + 6R + 7 \\ \lambda_2 = (R-1)^2 \\ \lambda_3 = (R-1)^2 \end{cases} \tag{6}$$

For spherical particles (R =1) this leads to zero entropy but for a cloud of 'wet dipoles' (m and ε_r large) the entropy rises to 0.95. Hence a measurement of entropy relates to information about composition of the volume. Importantly, we can estimate scattering entropy numerically on a pixel-by-pixel basis from quadpol radar imaging data. Figure 2b shows an example of the entropy or phase stability of a mixed scene, being the Oberpfaffenhofen area as collected by the DLR L-Band ESAR system. We note that over non-vegetated surfaces (left bottom corner in figure 2b) the entropy is low and hence the scattered wave helix is very stable for all types of transmit polarisation. This can be exploited for quantitative moisture and roughness estimation of non-vegetated land surfaces by choosing appropriate robust ratios of scattering elements as shown for example in table I. [10,11,12,13,14,15]

The urban areas (upper right corner) in figure 2 show moderate entropy, but the worst case arises for vegetation (lower right corner). Here we see high entropy due to volume scattering by the random components of the vegetation cover (as in equation 6). These observations are independent of the actual scene considered and hence have been suggested by several authors as suitable for robust unsupervised classification of land cover [3,4,5,13].

While useful for classification and limited composition studies, such high entropy for vegetation cover restricts our ability to fully exploit polarisation for quantitative parameter estimation. Yet vegetation cover is of prime importance in remote sensing applications. Somehow, in order to proceed, we have to find a way to reduce the entropy. Importantly this can be achieved by combining polarimetry with interferometry, to form the new topic of imaging polarimetric interferometry or POLInSAR as we now show.

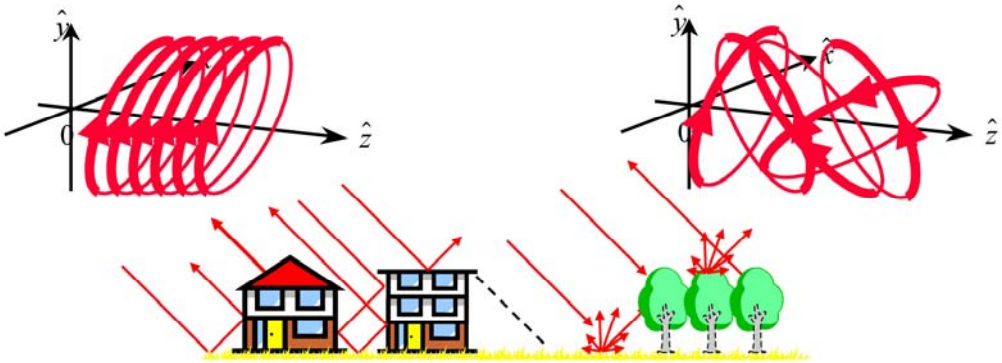

Figure 2a: Depolarisation and Entropy:

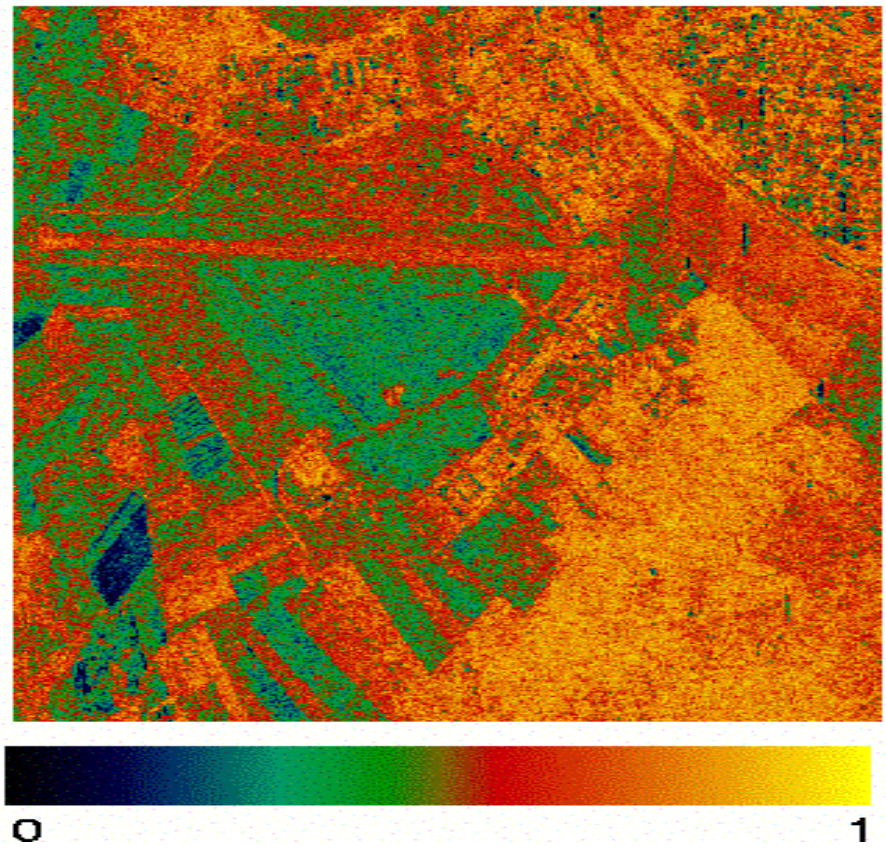

Figure 2b : Entropy image L-Band Oberpfaffenhofen, Germany DLR ESAR Data

Controlling Entropy : Volume Decorrelation in Radar Interferometry

Radar interferometry employs spatial separation by a baseline vector b of multiple sensors (for single-pass) or a single sensor at multiple times (for repeat-pass) [18]. It then uses phase difference as a proxy for elevation, enabling determination of scatterer height, hence leading to products such as high resolution digital elevation model (DEM) generation. Again however, the accuracy of this process is governed by phase stability or coherence. In this case we can define a coherency matrix as shown in equation 7

$$[J]_x = \begin{bmatrix} \langle p_x(\underline{r}) p_x^*(\underline{r}) \rangle & \langle p_x(\underline{r}) p_x^*(\underline{r}+\underline{b}) \rangle \\ \langle p_x(\underline{r}) p_x^*(\underline{r}+\underline{b}) \rangle & \langle p_x(\underline{r}+\underline{b}) p_x^*(\underline{r}+\underline{b}) \rangle \end{bmatrix} \tag{7}$$

where 'x' corresponds to a single selected polarisation channel. The presence of vegetation is now modelled as a finite bounded vertical random distribution of scatterers with a spatial weighting to account for the fact that scatterers deeper in the volume will have a smaller influence due to wave extinction. With this model, the coherence of vegetation can be expressed as shown in equation 8 [19,22]

$$\tilde{\gamma}_v e^{i\phi(z_o)} = \frac{\langle p_x(\underline{r}) p_x^*(\underline{r}+\underline{b}) \rangle}{\sqrt{\langle p_x(\underline{r}) p_x^*(\underline{r}) \rangle \cdot \langle p_x(\underline{r}+\underline{b}) p_x^*(\underline{r}+\underline{b}) \rangle}} = e^{i\phi(z_o)} \frac{2\sigma_1 e^{i\phi(z_o)}}{\cos\theta_o (e^{2\sigma_1 h_v/\cos\theta_o} - 1)} \int_0^h e^{ik_z z'} e^{\frac{2\sigma_1 z'}{\cos\theta_o}} dz'$$

$$= e^{i\phi(z_o)} \frac{\mathrm{p}_1}{p_2} \frac{e^{p_2 h_v} - 1}{e^{p_1 h_v} - 1} \qquad p_1 = \frac{2\sigma}{\cos\theta} \qquad p_2 = p_1 + ik_z, \qquad k_z = \frac{4\pi\Delta\theta}{\lambda \sin\theta} \approx \frac{4\pi B_n}{\lambda R \sin\theta} \tag{8}$$

where B_n is the normal component of the baseline to the line of sight. There are two key features of this model:

- Coherence (and therefore entropy) can now be controlled by selecting the baseline B_n.
- The interferometric coherence is independent of 'x' i.e. of polarisation

The first means that, unlike in polarimetry, we can now design the sensor to control the observed entropy of vegetation scattering (contrast equations 6 and 8). However, the second seems to indicate that we do not need polarisation diversity, as equation 8 does not change with 'x'. Why then do we need to consider POLInSAR? The answer to this apparent contradiction is hidden in equation 8 itself. We see that the coherence is a function of several parameters, the unknown height of the vegetation , the unknown wave extinction and the unknown ground topographic phase. It follows that one channel of interferometry by itself cannot be used for unambiguous parameter retrieval. The situation is further complicated by the fact that for microwaves the extinction can be relatively small and hence there can be penetration of vegetation right down to the underlying surface. This requires us to consider combined surface and volume scattering, so forcing us to modify equation 8 to at least a two-layer model as shown in equation 9 [19,20,21,22].

$$\tilde{\gamma}_x = e^{i\phi(z_o)} \frac{\tilde{\gamma}_v + \mu_x}{1 + \mu_x} \tag{9}$$

where μ_x is the ratio of surface-to-volume scattering, which changes with frequency, vegetation density and surface conditions. However, it is now that polarisation diversity helps, as from figure 2b we see that surface scattering has low entropy and hence we can control its influence in 9 by changing

'x' at the same time as leaving the volume coherence unchanged. Consequently by using POLInSAR we can increase the number of observations faster than the number of unknowns and hence achieve parameter estimation with a coherence or entropy under our control. This is one reason why there is such an interest in developing POLInSAR sensors for vegetation mapping [22,23,24]. Several further examples can be found as part of the proceedings of a recent ESA funded workshop focussing on this topic (http://earth.esa.int/polinsar/).

Figure 3 shows an example POLInSAR product, obtained using the L-band airborne E-SAR sensor operated by DLR in Germany. Here we show a radar-derived quantitative tree height estimation overlaid on a radar-derived DEM. It uses the model of equation 9 with polarisation diversity over 'x' to isolate the height h_v and $\varphi(z_0)$ dependence and provide a map of tree height over the mountainous terrain. Quantitative comparisons with in-situ measurements indicate an accuracy of height estimation around 10%. [21,22,24]. While tree height is itself a useful product, it can also provide the basis for various important secondary products. For example, in Figure 4 we show a forest biomass map derived using the height data in Figure 3 coupled to allometric equations derived from forestry tables for this region [24]. In the upper Figure we also show a conventional SAR image of the scene, which displays

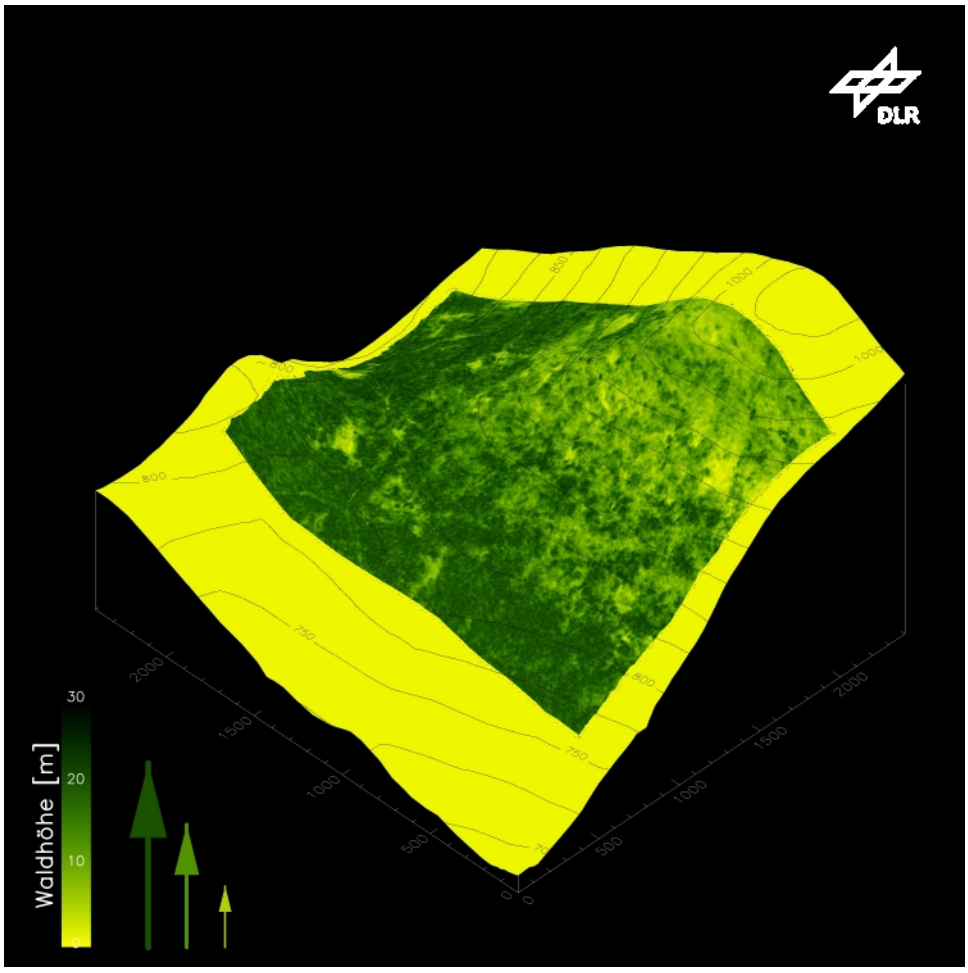

Figure 3: Tree Height and Topography Estimated using L-Band
DLR E-SAR Polarimetric Interferometric Data

none of the important forest structural information seen in the height/biomass products. This nicely illustrates the potential 'information gain' obtained by using POLInSAR sensors for vegetation applications.

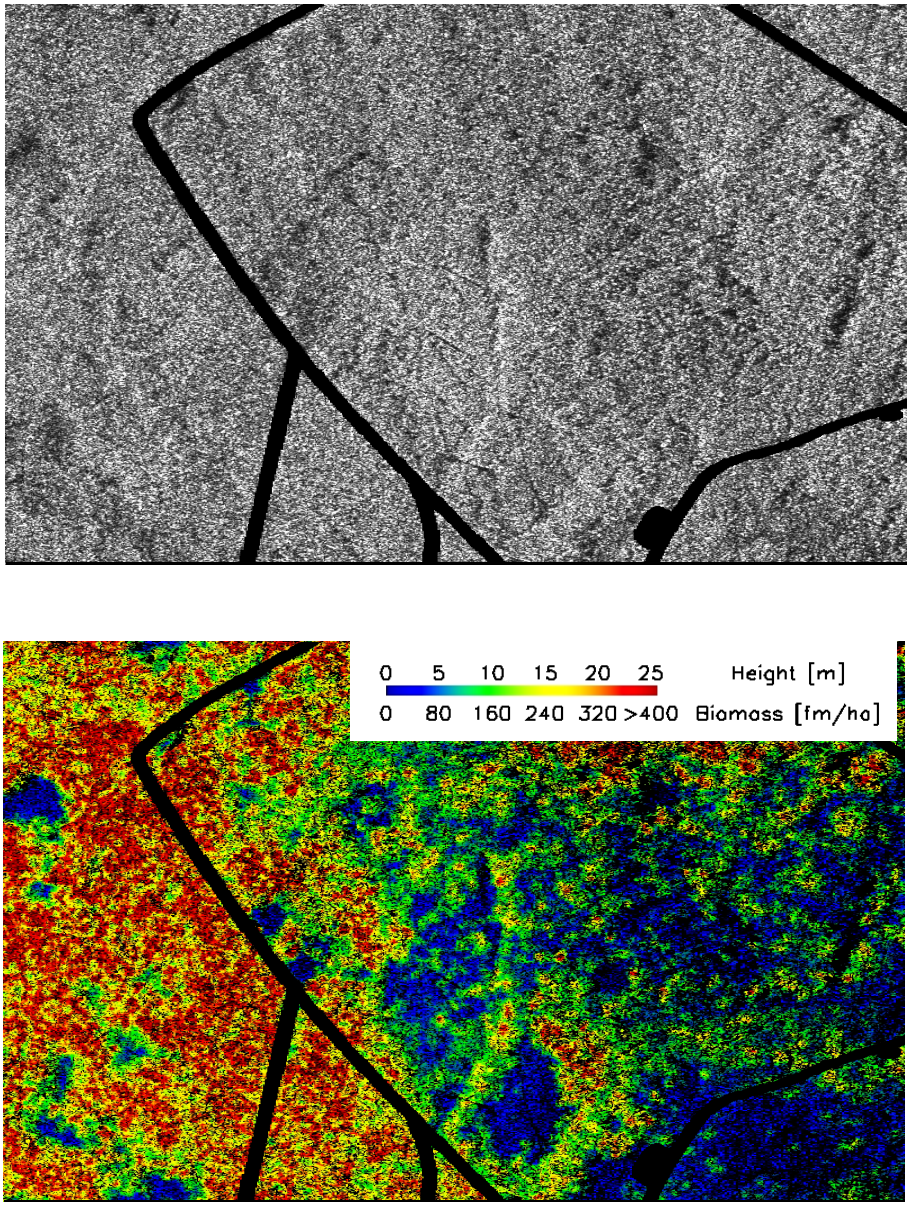

Figure 4 : HH RCS image (upper) and radar derived tree height/biomass map for the same scene (lower) (see reference [24])

Conclusions and Future Developments

In this treatment we have developed as a theme the importance of multi-channel phase in radar remote sensing and used it to support the idea of combining polarisation diversity with interferometry in future radar sensors. Key to success is the generalised coherence or entropy and key to robustness the development of physical models for the interaction of polarised waves with natural surfaces. We have concentrated on one important example, namely tree height and biomass estimation, but there are many other application areas where this technology is being considered. Table I provides a selective survey of different geo-physical parameters and examples of the types of algorithms currently being developed. We can see that polarimetric and/or interferometric phase appears in every area. This table

provides a 'snapshot' in time, each area is ongoing in research and development and exciting future technology innovations such as bistatic radar and satellite radar constellations will require parallel improvements in our understanding of the interaction of polarised waves with natural media in order to fully exploit the scientific and commercial potential of radar in remote sensing.

By using more than 2 polarimetric data sets polarimetric interferomerty can be extend to more complex approaches. One of possible approache is differential polarimetric interferometry. By using 3 or more temporal separated data sets it could be possible to enhance the potential of conventional differential interferometry by using the polarimetric information in order to analyse the changes in scattering processes over time. POL-IN-SAR imaging, when applied to 'Repeat-Pass Image Overlay Interferometry', provides differential background validation and measurement, stress assessment, and environmental stress-change monitoring capabilities.

Another approach currently under investigation is polarimetric SAR tomography, which is the extension of conventional two-dimensional SAR imaging principle to three dimensions. A real three-dimensional imaging of a scene is achieved by the formation of an additional synthetic aperture in elevation by a coherent cobination of images acquired from several parallel flight tracks. It can be seen as a direct approach to resolve the SAR scattering ambiguity problems. The introduction of tomographic SAR offers the possibility of a direct localisation and identification of all scattering contributions in a volume. This greatly extends the potential of SAR, particularly for the analysis of volume structures like for example forests as shown in Figure 5.

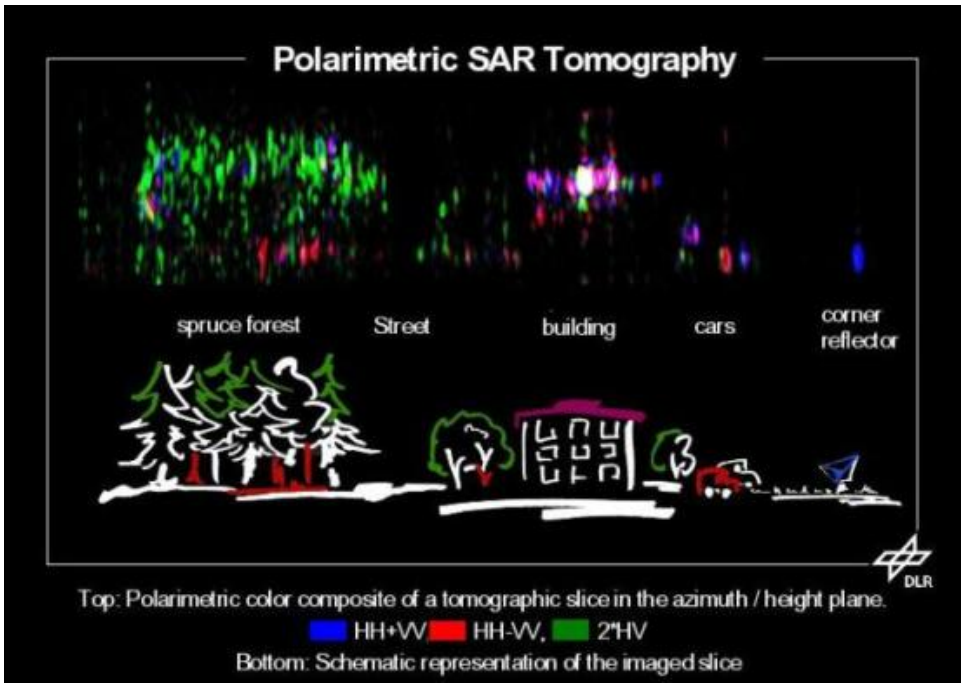

Figure 5 Tomographic slice generated from 13 parallel flight tracks with a mutual distance of 20m. Sensor: DLR ESAR in L-band. Scene: Onberpfaffenhofen, Germany. (Reigber[25])

Acknowledgements

Thank is due to Professor Eric Pottier of the University of Rennes, France, and Dr. Andreas Reigber from the Technical University of Berlin for their valuable assistance in composing this tutorial.

Product	Radar Parameter	Polarimetric and Interferometric Measurement Parameters	Source Ref.
Bare Surface Roughness	$0 \le R(ks) \le 1$ s=rms roughness k=wavenumber=$2\pi/\lambda$	$R = \dfrac{\left\langle \lvert S_{HH} - S_{VV} \rvert^2 \right\rangle - 4\left\langle \lvert S_{HV} \rvert^2 \right\rangle}{\left\langle \lvert S_{HH} - S_{VV} \rvert^2 \right\rangle + 4\left\langle \lvert S_{HV} \rvert^2 \right\rangle}$	10,11,15
Bare Surface Moisture	$0 \le M(\theta,\varepsilon_r) \le 1$ θ = angle of incidence ε_r – dielectric constant	$M = \dfrac{\left\langle \lvert S_{HH} - S_{VV} \rvert^2 \right\rangle + 4\left\langle \lvert S_{HV} \rvert^2 \right\rangle}{\left\langle \lvert S_{HH} + S_{VV} \rvert^2 \right\rangle}$	10,11,15
Surface Slope	$\tan\beta = \dfrac{\tan\omega}{\sin\bar{\phi} - \cos\bar{\phi}\tan\gamma}$ $\tan\gamma$ = range slope $\tan\omega$ = azimuth slope $\bar{\phi}$ = radar look angle	$\phi = \tan^{-1}\left(\dfrac{2\mathrm{Re}\left\langle (S_{HH} - S_{VV}).S_{HV}^{*} \right\rangle}{4\left\langle \lvert S_{HV} \rvert^2 \right\rangle - \left\langle \lvert S_{HH} + S_{VV} \rvert^2 \right\rangle}\right)$ $-\dfrac{\pi}{4} \le \beta = \begin{cases} \dfrac{\phi+\pi}{4} & \text{if } \phi \le \dfrac{\pi}{4} \\ \dfrac{\phi+\pi}{4} - \dfrac{\pi}{2} & \text{if } \phi > \dfrac{\pi}{4} \end{cases} \le \dfrac{\pi}{4}$	12,14
True Ground Topography	$z_o = z_{ref} + \dfrac{\hat{\phi}}{k_z}$ $k_z = \dfrac{4\pi\Delta\theta}{\lambda\sin\theta} \approx \dfrac{4\pi B_n}{\lambda R\sin\theta}$	$\hat{\phi} = \arg(\tilde{\gamma}_{HH-VV} - \tilde{\gamma}_{HV}(1-L))$ $A = \lvert\tilde{\gamma}_{HV}\rvert^2 - 1,$ $B = 2\mathrm{Re}((\tilde{\gamma}_{HH-VV} - \tilde{\gamma}_{HV}).\tilde{\gamma}_{HV}^{*}),$ $C = \lvert\tilde{\gamma}_{HH-VV} - \tilde{\gamma}_{HV}\rvert^2$ $AL^2 + BL + C = 0 \Rightarrow \hat{L}$	21,22,23
Vegetation Component Structure	$m = \begin{cases} >1 & \text{prolate particles} \\ 1 & \text{spherical particles} \\ <1 & \text{oblate particles} \end{cases}$ $P = \dfrac{m\varepsilon_r + 2}{m + \varepsilon_r + 1}$	$V = \dfrac{4\left\langle \lvert S_{HV} \rvert^2 \right\rangle}{\left\langle \lvert S_{HH} + S_{VV} \rvert^2 \right\rangle}$ $\Rightarrow a = (1-2V), b = -2(1+3V), c = (1-7V)$ $\Rightarrow aP^2 + bP + c = 0 \Rightarrow \hat{P}$	4,16,17
Vegetation Height and Extinction	h_v = top height in m σ = mean extinction (m^{-1}) θ = angle of incidence $\hat{\phi}$ = ground topographic phase (see above)	$\min_{h_v,\sigma} L_1 = \left\lVert \tilde{\gamma}_{HV} - e^{i\hat{\phi}} \dfrac{p}{p_1} \dfrac{e^{p_1 h_v} - 1}{e^{p h_v} - 1} \right\rVert$ where $\begin{cases} p = \dfrac{2\sigma}{\cos\theta} \\ p_1 = p + ik_z \end{cases}$	20,21,22

Table I : Examples of Geophysical Parameter Estimation using Radar Polarimetry and Interferometry

References

[1] Boerner W M et al “Polarimetry in Remote Sensing: Basic and Applied Concepts”, Chapter 5 in Manual of Remote Sensing, Vol. 8, 3rd edition, F M Henderson, A J Lewis eds. New York, Wiley, 1998

[2] Cloude S R, E. Pottier, "A Review of Target Decomposition Theorems in Radar Polarimetry", IEEE Transactions on Geoscience and Remote Sensing, Vol. 34 No. 2, pp 498-518, March 1996

[3] Freeman A, S.L. Durden, “A Three Component Model for Polarimetric SAR Data”, IEEE Transactions on Geoscience and Remote Sensing, Vol. GE-36, pp. 963-973, 1998

[4] Cloude S R, E. Pottier, "An Entropy Based Classification Scheme for Land Applications of Polarimetric SAR", IEEE Transactions on Geoscience and Remote Sensing, Vol. 35, No. 1, pp 68-78 , January 1997

[5] van Zyl J J "Unsupervised Classification of Scattering Behaviour Using Radar Polarimetry Data", IEEE Transactions on Geoscience and Remote Sensing, Vol. GE-27(1), 1990, pp 36-45

[6] Born M, E Wolf "Principles of Optics", Chapters 1, 10, Pergamon Press, 6th Edition, 1989, ISBN 0-08-026428-4

[7] Touzi R, A Lopes, J Bruniquel, P W Vachon,“Coherence Estimation for SAR Imagery”, IEEE Transactions Geoscience and Remote Sensing, Vol. 37/1, pp 135-149, January 1999

[8] Freeman A., S Saatchi, “Effects of Faraday Rotation on Backscatter Signatures in SAR Image data”, Proc. SPIE, vol 3120, pp 37-44, 1997

[9] Quegan S “A Unified Algorithm for Phase and Cross-talk calibration of Polarimetric Data-theory and Observations”, IEEE Trans GRS-32, Jan 1994, pp 89-99

[10] Hajnsek I., E. Pottier, S.R. Cloude”, Inversion of Surface Parameters from Polarimetric SAR”, IEEE Transactions on Geoscience and Remote Sensing, Vol 41/4, April 2003, pp 727-744

[11] Hajnsek I., Papathanassiou, K. P. & Cloude, S. R., ‘Surface Parameter Estimation Using fully polarimetric L- and P-band Radar data’, Proc. 3rd International Symposium, ‘Retrieval of Bio-Geophysical Parameters from SAR Data for Land Applications’, 11-14 Sept. 2001, Sheffield, UK, ESA SP-475, January 2002, pp. 159-164

[12] Lee J.S., D L Schuler, T L Ainsworth, “Polarimetric SAR Data Compensation for Terrain Azimuth Slope Variation”, IEEE Trans. Geoscience and Remote Sensing, Vol 38/5, pp 2153-2163, September 2000

[13] Lee J.S., M.R. Grunes, T.L .Ainsworth, L. J. Du, D. L. Schuler, S.R Cloude, “Unsupervised Classification using Polarimetric Decomposition and the Complex Wishart Distribution”, IEEE Transactions Geoscience and Remote Sensing, Vol 37/1, No. 5, p 2249-2259, September 1999

[14] Schuler D, T. Ainsworth, J.S. Lee, G. De Grandi, "Topographic Mapping using Polarimetric SAR data”, International Journal of Remote Sensing, Vol. 34, no. 5, pp 1266-1277, 1998

[15] Cloude S.R., D G Corr, “A New Parameter for Soil Moisture Estimation”, Proceedings of IEEE International Geoscience and Remote Sensing Symposium (IGARSS 2002), Toronto, Canada, Vol. 1, pp 641-643, July 2002

[16] Cloude S.R., J. Fortuny, J.M. Lopez, A. J. Sieber, “Wide Band Polarimetric Radar Inversion Studies for Vegetation Layers”, IEEE Transactions on Geoscience and Remote Sensing, Vol 37/2 No 5, pp 2430-2442, September 1999

[17] Cloude S R, "Helicity in Radar Remote Sensing", Proceedings of IEEE International Geoscience and Remote Sensing Symposium (IGARSS 2002), Toronto, Canada, Vol.1, pp 411-413, July 2002

[18] Bamler R, P. Hartl, "Synthetic Aperture Radar Interferometry", Inverse Problems, 14, R1-R54, 1998

[19] Treuhaft R N, P. Siqueria, "Vertical Structure of Vegetated Land Surfaces from Interferometric and Polarimetric Radar", Radio Science, Vol. 35(1), pp 141-177, January 2000

[20] Cloude S R, K P Papathanassiou, "Polarimetric SAR Interferometry", IEEE Transactions on Geoscience and Remote Sensing, Vol 36. No. 5, pp 1551-1565, September 1998

[21] Papathanassiou K.P., S.R. Cloude, "Single Baseline Polarimetric SAR Interferometry", IEEE Transactions Geoscience and Remote Sensing, Vol 39/11, pp 2352-2363, November 2001

[22] Cloude S.R. , K.P. Papathanassiou, " A 3-Stage Inversion Process for Polarimetric SAR Interferometry", IEE Proceedings, Radar, Sonar and Navigation, Volume 150, Issue 03, June 2003, pp 125-134

[23] Yamada H, Y Yamaguchi, E Rodriguez, Y Kim, W M Boerner, "Polarimetric SAR Interferometry for Forest Canopy Analysis by Using the Super-resolution Method", IEICE Transactions on Electronics, VOL.E84-C, No.12, 2001, pp1917-1924, December 2001

[24] Mette T., I. Hajnsek, K. P. Papathanassiou, R Zimmerman, " Above Ground Forest Biomass Estimation using Fully Polarimetric/Interferometric Radar Data", Proceedings of ESA Workshop, POLInSAR – Applications of SAR Polarimetry and Polarimetric Interferometry, Frascati, Italy, January 2003, SP-529, http://www.earth.esa.int/polinsar

[25] Reigber A.,"Airborne Polarimetric SAR Tomography", DLR Report No. 2002-2, PhD thesis University of Stuttgart, Germany 2001

[26] Gerhard Krieger, Kostas Papathanassiou, Shane Cloude, Alberto Moreira, Hauke Fiedler, Michael Všlker, "Spaceborne Polarimetric SAR Interferometry: Performance Analysis and Mission Concepts", Proceedings of 2nd ESA POLInSAR Workshop, Frascati, January 2005, http://earth.esa.int/workshops/polinsar2005/

[27] K.P. Papathanassiou, S.R. Cloude , A Liseno, T. Mette , and H. Pretzsch,Forest, "Height Estimation by means of Polarimetric SAR Interferometry: Actual Status and Perspectives", Proceedings of 2nd ESA POLInSAR Workshop, Frascati, Italy, January 2005, http://earth.esa.int/workshops/polinsar2005/

[28] S. R. Cloude , M. L. Williams, "Estimating sub-canopy soil moisture using POLInSAR", Proceedings of 2nd ESA POLInSAR Workshop, Frascati, January 2005, http://earth.esa.int/workshops/polinsar2005/

[29] Tobias Mette, "Performance of Forest Biomass Estimation from Pol-InSAR and Forest Allometry over Temperate Forests", Proceedings of 2nd ESA POLInSAR Workshop, Frascati, January 2005, http://earth.esa.int/workshops/polinsar2005/